

DOI: 10.1002/chem.201301788

Luminescent Amphiphilic 2,6-Bis(1,2,3-triazol-4-yl)pyridine–Platinum(II) Complexes: Synthesis, Characterization, Electrochemical, Photophysical, and Langmuir–Blodgett Film-Formation Studies

Yongguang Li,^[a, b] Le Zhao,^[a, b] Anthony Yiu-Yan Tam,^[b] Keith Man-Chung Wong,^{*[b, c]}
Lixin Wu,^{*[a]} and Vivian Wing-Wah Yam^{*[a, b]}

Abstract: A new series of platinum(II) complexes with tridentate ligands 2,6-bis(1-alkyl-1,2,3-triazol-4-yl)pyridine and 2,6-bis(1-aryl-1,2,3-triazol-4-yl)pyridine (N7R), [Pt(N7R)Cl]X (**1–7**) and [Pt(N7R)(C≡CR')X] (**8–17**; R = *n*-C₄H₉, *n*-C₈H₁₇, *n*-C₁₂H₂₅, *n*-C₁₄H₂₉, *n*-C₁₈H₃₇, C₆H₅, and CH₂-C₆H₅; R' = C₆H₅, C₆H₄-CH₃-*p*, C₆H₄-CF₃-*p*, C₆H₄-N(CH₃)₂-*p*, and cholesteryl 2-propyn-1-

yl carbonate; X = OTf⁻, PF₆⁻, and Cl⁻), has been synthesized and characterized. Their electrochemical and photophysical properties have also been studied. Two amphiphilic platinum(II)–

Keywords: amphiphiles • interfaces • Langmuir–Blodgett films • luminescence • platinum

2,6-bis(1-dodecyl-1,2,3-triazol-4-yl)pyridine complexes (**3-Cl** and **8**) were found to form stable and reproducible Langmuir–Blodgett (LB) films at the air/water interface. These LB films were characterized by the study of their surface-pressure–molecular-area (π -A) isotherms, XRD, and IR and polarized-IR spectroscopy.

Introduction

Over the past few decades, the spectroscopic and photophysical behavior of square-planar d⁸ platinum(II) complexes have been widely investigated, owing to their intriguing spectroscopic and luminescence properties.^[1–5] Platinum(II)–terpyridine (tpy) complexes have attracted much attention in recent years, mainly due to their square-planar structures and their propensity to exhibit non-covalent Pt··Pt interactions and π - π -stacking interactions of the terpyridine ligands.^[2a–g, 3a–e, k, l] As a representative example, the chloroplatinum(II)–terpyridine complex was found to show strong luminescence in the solid state,^[3a–c] but was found to be non-emissive in solution at room temperature, owing to non-radiative deactivation through the low-lying d–d ligand-field (LF) state.^[3a, b, d, e, k–m]

Recently, luminescent alkynylplatinum(II)–terpyridine complexes that emit in solution at room temperature have been reported.^[2a] Apart from introducing intraligand (IL) character into the excited state of platinum(II) complexes through the incorporation of extended π -conjugated ligands, as demonstrated by McMillin and co-workers,^[3e, m, n] Yam and co-workers showed that substitution of the weak-field chloro ligand by a stronger-field alkynyl ligand would lead to a larger d–d orbital splitting, thereby raising the energy of the non-emissive d–d ligand-field excited state and giving rise to an emission that arises from the triplet excited state, which shows metal-to-ligand charge-transfer (MLCT) [$d\pi(\text{Pt}) \rightarrow \pi^*(\text{tpy})$] and some ligand-to-ligand charge-transfer (LLCT) [$\pi(\text{C}\equiv\text{C}) \rightarrow \pi^*(\text{tpy})$] character. These alkynylplatinum(II)–terpyridine complexes also showed drastic changes in their spectroscopic and luminescence properties upon changes in the microenvironment in the presence of external stimuli, including a change in the solvent composition,^[2b, c] counteranion,^[2c, 4a] polymer,^[2d, l, m] pH value,^[5c–e] ion binding,^[5a–c] and biomolecule interactions.^[2f, 5g] Extensions of this work to dinuclear complexes with a flexible bridge^[2g, o, p] and metallogel formation,^[2n, o, 4a, b, f] which involved interesting color changes as a result of intramolecular and intermolecular assembly/disassembly processes through Pt··Pt and π - π interactions, have also been reported.

Another tridentate N-donor ligand, 2,6-bis(benzimidazolyl)pyridine, has also been reported to coordinate to platinum(II) center to form chloroplatinum(II) complexes.^[6] This type of amphiphilic complexes were found to show Langmuir–Blodgett film-forming properties. Apart from being emissive in the solid state, both the monolayer and the multilayer LB films showed luminescence. Their aggregation^[6a–c]

[a] Dr. Y. Li, Dr. L. Zhao, Prof. Dr. L. Wu, Prof. Dr. V. W.-W. Yam
State Key Laboratory of Supramolecular Structure and
Materials and College of Chemistry
Jilin University, Changchun 130012 (P. R. China)
E-mail: wulx@jlu.edu.cn
wyyam@hku.hk

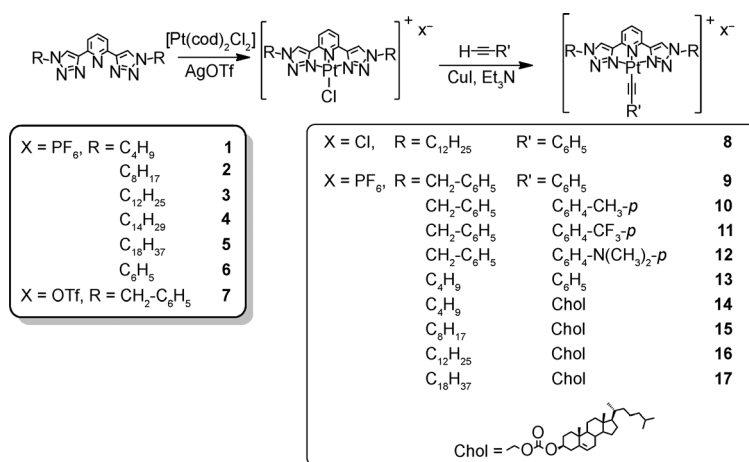
[b] Dr. Y. Li, Dr. L. Zhao, Dr. A. Y.-Y. Tam, Dr. K. M.-C. Wong,
Prof. Dr. V. W.-W. Yam
Institute of Molecular Functional Materials
and Department of Chemistry
The University of Hong Kong, Pokfulam Road (Hong Kong)
E-mail: wongmc@hku.hk

[c] Dr. K. M.-C. Wong
Current address:
Department of Chemistry
South University of Science and Technology of China
1088 Xueyuan Blvd., Shenzhen 518055 (P. R. China)

and Förster resonance energy transfer (FRET)^[6d] properties have also been studied. By employing a similar synthetic approach to that for alkynylplatinum(II)–terpyridine complexes, a related class of luminescent 2,6-bis(*N*-alkylbenzimidazol-2-yl)pyridine–alkynylplatinum(II) complexes has been synthesized and shown to exhibit a dual-luminescence behavior in solution, which was sensitive to the polarity of the solvent, as well as metallogelation properties.^[4c,6e]

Apart from the terpyridine and 2,6-bis(benzimidazolyl)pyridine systems, chloro- and alkynylplatinum(II) complexes of other tridentate N-donor ligands, such as 2,6-bis(1-alkylpyrazol-3-yl)pyridine, have been synthesized and shown to display reproducible Langmuir–Blodgett film-forming properties and good charge-transport properties.^[7] In addition, chloroplatinum(II) and phenylplatinum(II) complexes of 2,6-bis(pyrazol-1-yl)pyridine and 2,6-bis(3,5-dimethylpyrazol-1-yl)pyridine have been prepared by Connick and co-workers.^[8] Similar to the chloroplatinum(II)–terpyridine system, some of these complexes were shown to exhibit very weak emission, probably as a result of non-radiative deactivation through the low-lying d–d ligand-field (LF) state.

Similar to the tridentate 2,6-bis(pyrazol-1-yl)pyridine and 2,6-bis(pyrazol-3-yl)pyridine ligands, another new class of tridentate N-donor ligand, 2,6-bis(1,2,3-triazol-4-yl)pyridine, has been investigated in d-block transition-metal complexes and f-block lanthanides over the past few decades, including zinc(II),^[9] europium(III),^[9a,b,10] iron(II),^[9,10] and ruthenium(II).^[9,11] However, the related platinum(II) complexes of 2,6-bis(1,2,3-triazol-4-yl)pyridine have not been explored. Herein, we report a series of 2,6-bis(1-alkyl-1,2,3-triazol-4-yl)pyridine and 2,6-bis(1-aryl-1,2,3-triazol-4-yl)pyridine platinum(II) complexes, [Pt(N7R)Cl]X (**1–7**) and [Pt(N7R)(C≡CR')]X (**8–17**; N7R = 2,6-bis(1-alkyl-1,2,3-triazol-4-yl)pyridine or 2,6-bis(1-aryl-1,2,3-triazol-4-yl)pyridine; R = *n*-C₄H₉, *n*-C₈H₁₇, *n*-C₁₂H₂₅, *n*-C₁₄H₂₉, *n*-C₁₈H₃₇, C₆H₅, and CH₂-C₆H₅; R' = C₆H₅, C₆H₄-CH₃-*p*, C₆H₄-CF₃-*p*, C₆H₄-N(CH₃)₂-*p*, and cholesteryl 2-propyn-1-yl carbonate; X = OTf⁻, PF₆⁻, and Cl⁻), with different groups on the nitrogen atom of the triazole units (Scheme 1). Their electrochemical and photophysical properties have been studied. Two amphiphilic platinum(II) complexes that contained two dodecyl chains (**3-Cl** and **8**) have been found to form stable and reproducible Langmuir–Blodgett (LB) films at the air/water interface.



Scheme 1. Synthesis of complexes **1–17**. cod = 1,5-cyclooctadiene.

Results and Discussion

Synthesis and characterization: Cholesteryl 2-propyn-1-yl carbonate was synthesized according to literature procedures.^[4d] The 2,6-bis(1-alkyl-1,2,3-triazol-4-yl)pyridine and 2,6-bis(1-aryl-1,2,3-triazol-4-yl)pyridine ligands were synthesized from the click reactions of 2,6-diethynylpyridine with their corresponding aliphatic or aryl azides in the presence of a catalytic amount of copper(II) sulfate pentahydrate and sodium ascorbate.^[10] Chloroplatinum(II) complexes **1–7** were obtained by the modification of previously reported literature procedures for the synthesis of the related chloroplatinum(II) complexes of 2,6-bis(benzimidazolyl)pyridine^[6e] and 2,6-bis(1-alkylpyrazol-3-yl)pyridine.^[7a] Alkynylplatinum(II) complexes **8–17** were prepared by the reaction of their corresponding chloroplatinum(II) complexes with various organic alkynes in the presence of a catalytic amount of copper(I) iodide and triethylamine in CH₂Cl₂. The identities of all of the newly synthesized complexes were confirmed by ¹H NMR spectroscopy, FAB mass spectrometry and satisfactory elemental analyses.

Electrochemistry: The electrochemical behavior of these complexes was studied by using cyclic voltammetry. In general, the cyclic voltammograms of these complexes in CH₂Cl₂ in the presence of *n*Bu₄NPF₆ (0.1 M) as a supporting electrolyte displayed a quasi-reversible reduction couple, irreversible reduction waves from about –1.14 to –1.37 V and from –1.81 to –1.91 V, respectively, and an irreversible anodic wave from approximately +0.63 to +1.89 V (versus SCE). The electrochemical data for selected complexes are summarized in Table 1. Owing to the sensitivity of the potential of the oxidation wave towards the electronic effect of the alkynyl ligand, the irreversible oxidation wave was attributed to the oxidation of Pt^{II} into Pt^{III}, with substantial mixing of the character of the alkynyl ligand. This assignment was in agreement with the observation that the ease of oxidation increased in the order: **11** (+1.89 V) < **9** (+1.57 V) < **10** (+1.28 V) < **12** (+0.63 V), which was in line

Table 1. Electrochemical data for selected complexes.^[a]

Complex	Oxidation E_{pa} (V vs. SCE) ^[b]	Reduction $E_{1/2}$ (V vs. SCE) ^[c]
3	— ^[d]	−1.14, −1.82 ^[e]
7	— ^[d]	−1.27, −1.88 ^[e]
8	+1.52	−1.37, −1.91 ^[e]
9	+1.57	−1.33, −1.91 ^[e]
10	+1.28	−1.27, −1.80 ^[e]
11	+1.89	−1.31, −1.85 ^[e]
12	+0.63	−1.21, −1.81 ^[e]
13	+1.49	−1.21, −1.82 ^[e]

[a] In CH_2Cl_2 with 0.1 M $n\text{Bu}_4\text{NPF}_6$ as a supporting electrolyte at RT; scan rate: 100 mV s^{-1} . [b] E_{pa} refers to the anodic peak potential for the irreversible oxidation wave. [c] $E_{1/2} = (E_{pa} + E_{pc})/2$; E_{pa} and E_{pc} are the peak anodic and cathodic potentials, respectively. [d] No oxidation wave. [e] Irreversible reduction wave.

with the order of the electron-donating ability of the substituent on the phenyl alkynyl ligands, NMe_2 (**12**) > CH_3 (**10**) > H (**9**) > CF_3 (**11**). On the basis of the similar potentials for the reduction couples of the chloroplatinum(II) and alkynylplatinum(II) complexes, as well as the relative insensitivity of the potentials toward the nature of the alkynyl ligands with different substituents, the reduction couples were mainly assigned to the ligand-centered reductions of the tridentate ligands.

Photophysical properties: The electronic absorption spectra of the complexes in CH_2Cl_2 or MeCN at 298 K showed intense absorption bands at 254–324 nm and moderately intense absorption bands at 354–504 nm. The photophysical data of the complexes are summarized in Table 2. With reference to previous spectroscopic work on the related platinum(II) complexes of terpyridine,^[2h] 2,6-bis(*N*-alkylbenzimidazol-2-yl)pyridine,^[6] and 2,6-bis(1-alkylpyrazol-3-yl)pyridine,^[7] as well as that of the tridentate (N7R) ligand,^[9b,c] the intense high-energy absorption bands, with extinction coefficients (ϵ) in the order of $10^4 \text{ dm}^3 \text{ mol}^{-1} \text{ cm}^{-1}$, were assigned as intraligand (IL) [$\pi \rightarrow \pi^*$] transitions of the N7R moieties and alkynyl ligands, whereas the low-energy absorption band at 356–364 nm in the spectra of chloroplatinum(II) complexes **1**, **3**, and **7**, with extinction coefficients (ϵ) in the order of $10^3 \text{ dm}^3 \text{ mol}^{-1} \text{ cm}^{-1}$, was tentatively assigned as the metal-to-ligand charge-transfer (MLCT) [$d\pi(\text{Pt}) \rightarrow \pi^*(\text{N7R})$] transition. However, for the alkynylplatinum(II) complexes, the moderately intense low-energy absorption bands were tentatively assigned as an admixture of metal-to-ligand charge-transfer (MLCT) [$d\pi(\text{Pt}) \rightarrow \pi^*(\text{N7R})$] and ligand-to-ligand charge-transfer (LLCT) [$\pi(\text{C}\equiv\text{C}) \rightarrow \pi^*(\text{N7R})$] transitions. This MLCT/LLCT assignment was further supported by the trend in the low-energy absorption bands: **11** (408 nm) > **9** (425 nm) > **10** (430 nm) > **12** (504 nm), which

Table 2. Electronic absorption and emission data of the complexes.

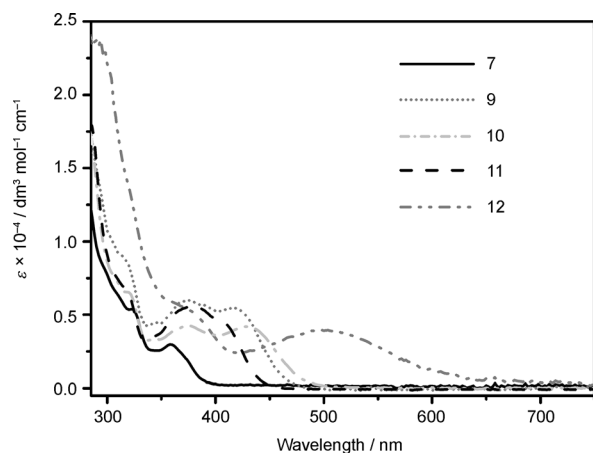
Complex	Medium	λ_{max} [nm] (ϵ_{max} [$\text{dm}^3 \text{ mol}^{-1} \text{ cm}^{-1}$])	Emission λ_{max} [nm] (τ_o [μs])
1	CH_3CN	276 (16920), 320 (6300), 354 (3960)	— ^[a]
	(298)		
3	CH_2Cl_2	280 (16240), 324 (5320), 360 (4050)	— ^[a]
	(298)		
7	CH_2Cl_2	280 (13800), 322 (5380), 358 (2980)	— ^[a]
	(298)		
8	solid (298)		585 (0.11)
	solid (77)		598 (2.19)
9	CH_2Cl_2	254 (58420), 284 (30690), 318 sh (7900), 366 (5590), 412 (4530)	573 (<0.1)
	(298)		
10	solid (298)		606 (0.25)
	solid (77)		640 (3.13)
11	CH_2Cl_2	260 (53170), 282 (14540), 318 sh (7900), 370 (5910), 425 sh (5210)	582 (<0.1)
	(298)		
12	solid (298)		600 (0.36)
	solid (77)		613 (1.60)
13	CH_2Cl_2	260 (36690), 284 sh (18980), 322 sh (6400), 374 (4270), 430 (4200)	591 (<0.1)
	(298)		
14	solid (298)		596 (0.54)
	solid (77)		618 (2.22)
15	CH_2Cl_2	262 (37590), 280 (18820), 318 sh (6690), 378 (5540), 408 (4500)	597 (<0.1)
	(298)		
16	solid (298)		620 (0.67)
	solid (77)		635 (1.85)
17	CH_2Cl_2	262 (24810), 288 (28830), 380 sh (5120), 504 (3950)	— ^[a]
	(298)		
18	solid (298)		715 (2.09)
	solid (77)		596 (<0.1)
19	CH_2Cl_2	260 (33570), 285 (14960), 320 sh (6060), 370 (4840), 420 (4360)	596 (<0.1)
	(298)		
20	solid (298)		656 (0.23)
	solid (77)		660 (5.49)
21	CH_2Cl_2	259 (20360), 279 (14750), 321 (5250), 366 (4640)	597 (<0.1)
	(298)		
22	solid (298)		631 (0.96)
	solid (77)		649 (1.73)
23	CH_2Cl_2	259 (20270), 280 (14600), 321 (4970), 366 (4530)	608 (<0.1)
	(298)		
24	solid (298)		625 (0.92)
	solid (77)		630 (1.53)

Table 2. (Continued)

Complex	Medium	λ_{\max} [nm] (ϵ_{\max} [dm ³ mol ⁻¹ cm ⁻¹])	Emission λ_{\max} [nm] (τ_o [μ s])
16	CH ₂ Cl ₂ (298)	259 (20040),	599 (<0.1)
		280 (14280),	
		321 (4900),	
		366 (4470)	
solid (298)	602 (0.78)		
	solid (77)	617 (1.11)	
17	CH ₂ Cl ₂ (298)	259 (20140),	605 (<0.1)
		279 (14430),	
		321 (4880),	
		366 (4390)	
	solid (298)	620 (0.74)	
solid (77)	627 (1.28)		

[a] Non-emissive.

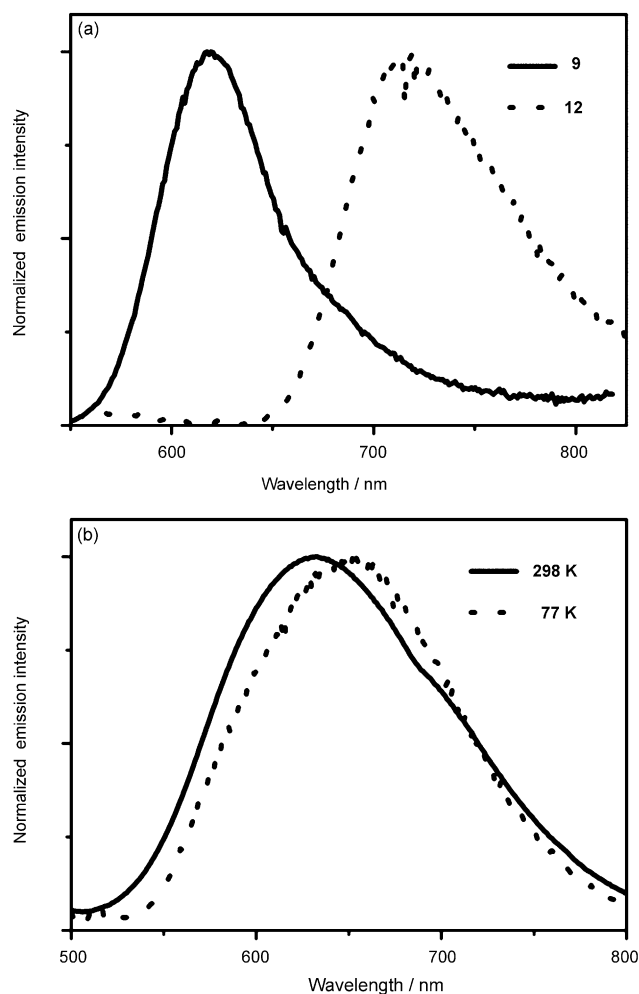
was consistent with the order of the electron-donating ability of the substituent on the ethynylbenzene ligand: NMe₂ (**12**) > CH₃ (**10**) > H (**9**) > CF₃ (**11**). Compared with chloroplatinum(II) complex **7**, the red-shift of the low-energy absorption band in the alkynylplatinum(II) complexes **9–12** was attributed to the raising of the HOMO energy level as a result of the presence of the stronger σ - and π -donating alkynyl group (Figure 1).

Figure 1. Electronic absorption spectra of complexes **7** and **9–12** in CH₂Cl₂ at room temperature.

Complexes **1–7** were found to be non-emissive in CH₂Cl₂ at room temperature. A probable reason for this lack of luminescence behavior is that the ³MLCT state would be quenched by the thermally accessible low-lying ³d–d ligand-field (LF) excited state through non-radiative decay. A similar observation has been reported in related platinum(II)–terpyridine systems.^[3a,b] On the contrary, the alkynylplatinum(II) complexes were found to be emissive and the luminescence data of complexes **8–17** are summarized in Table 2. The large Stokes shifts and the observed emission lifetimes within the microsecond range were suggestive of an origin

of triplet parentage. In CH₂Cl₂ at room temperature, alkynylplatinum(II) complexes **9–11** exhibited an emission at about 582–597 nm (Table 2). The emission energies of the complexes were found to be rather insensitive towards the nature of the substituents on the arylalkynyl ligand, thus suggesting that the emission predominantly originated from [$d_z^2(\text{Pt}) \rightarrow \pi^*(\text{N7R})$] MLCT excited-state character.

All of the alkynylplatinum(II) complexes were emissive in the solid state at room temperature and at 77 K, with the exception of complex **12**, which only emitted at 77 K (Table 2 and Figure 2). The lack of emissive behavior of complex **12**

Figure 2. a) Solid-state emission spectra of complexes **9** and **12** at 77 K. b) Solid-state emission spectra of complex **14** at 298 and 77 K.

at 298 K may be ascribed to photoinduced electron transfer (PET), which causes the quenching of the emissive ³MLCT excited state as a result of the electron that is transferred from the electron-rich amino group onto the platinum(II)–2,6-bis(1-benzyl-1,2,3-triazol-4-yl)pyridine moiety. Similar non-emissive behavior has been observed in related platinum(II)–terpyridine complexes with electron-donating meth-

oxy or amino substituents on the phenyl ring of the alkynyl group.^[2a-c,5a,d,g]

Langmuir–Blodgett films: For comparison with complex **8**, the PF₆⁻ counteranion of complex **3** was exchanged for Cl⁻ to give complex **3-Cl**, so as to eliminate the effects of the counteranion on the two complexes. To investigate the amphiphilic properties of complexes **3-Cl** and **8**, which contained two long C₁₂H₂₅ alkyl chains on the triazole units, these complexes were subjected to Langmuir–Blodgett (LB) film-formation studies. The surface-pressure–molecular-area (π -A) isotherms of complexes **3-Cl** and **8** are shown in Figure 3. The π -A isotherms of complexes **3-Cl** and **8**

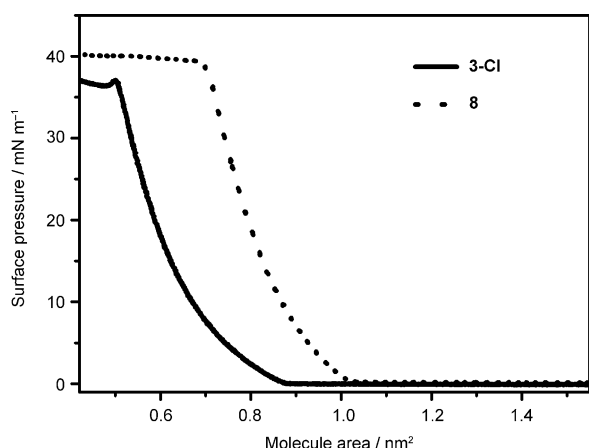


Figure 3. Surface-pressure–molecular-area isotherm of complexes **3-Cl** and **8** on a pure-water subphase at 20°C.

showed one well-defined condensed region with collapse pressures of 36–40 mNm⁻¹, thus suggesting that the complexes exhibited good and stable air/water interface behavior. Notably, these two complexes have similar π -A isotherms and fairly high collapse pressures as a result of the similarity between their structures. By extrapolating the plot in the condensed region to zero pressure, limiting molecular areas of 0.87 and 0.95 nm² were estimated for complexes **3-Cl** and **8**, respectively, thus suggesting that the coordination planes of the square-planar platinum(II) complexes were stacked adjacent to each other, with the long alkyl chains vertically oriented with respect to the water surface in an “edge-on” orientation, rather than a “flat-on” arrangement.

Multilayer LB films of complexes **3-Cl** and **8** were prepared on the glass substrates by using the Y-type deposition method. The transfer ratios in both the dipping and lifting processes were found to be constant and almost the same (approaching unity). Because small-angle XRD is a useful tool for estimating the molecular ordering, as well as the molecular orientation, in LB films on solid substrates, small-angle XRD was performed on an 85-layer-thick Y-type LB film of complex **8** that was prepared at 35 mNm⁻¹. Second-order diffractions were observed in the XRD patterns of the LB film at 20°C (Figure 4), thus indicating a layered struc-

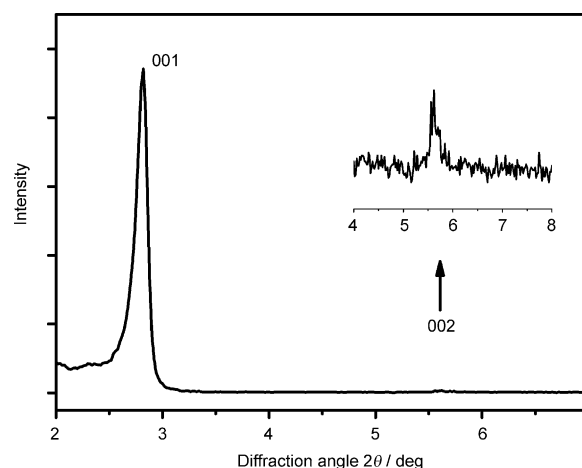


Figure 4. XRD patterns of an 85-layer-thick LB film of complex **8** that was transferred at a surface pressure of 35 mNm⁻¹ at 20°C.

ture. A sharp (001) Bragg diffraction was observed at $2\theta = 2.82^\circ$ and a layer distance (*d* spacing) of 3.13 nm was calculated by using Bragg’s equation. Such a value further supports an edge-on orientation, in which the long alkyl chains are tilted away from the normal of the glass substrate after the transfer.

To obtain more structural information, based on the sensitivity of the vibrational modes towards the molecular structure and dynamics of the alkyl chains,^[12] FTIR spectroscopy was employed to probe the structure of multilayer LB films of complex **8** at room temperature. As shown in Figure 5a, the absorption bands at 2920 and 2850 cm⁻¹ were assigned to antisymmetric and symmetric stretching vibrations of the CH₂ group, respectively. It is known that the frequencies of CH₂ stretches are sensitive towards the conformation of the alkyl chains. Low wavenumbers (2915–2920 and 2846–2850 cm⁻¹) are characteristic of a highly ordered (*trans* zigzag) conformation of the alkyl chains, whereas their upward shifts to higher frequencies (2924–2928 and 2854–2856 cm⁻¹) are indicative of an increase in conformational disorder (*gauche*) in the alkyl chains.^[13] Accordingly, the observed absorptions at 2920 and 2850 cm⁻¹ revealed the presence of highly ordered alkyl chains, whereas the absorption band at 1467 cm⁻¹ was typical of a CH₂ scissoring bending mode, which has been widely employed for the diagnosis of alkyl-chain packing.^[14] Based on the IR and polarized-IR absorption spectra,^[15] the molecular orientation in the thin film could be determined. The calculated mean tilting angle of the alkyl chains was determined to be about 18°, based on the linear relationship of the diagnostic bands (Figure 5b). In view of the fact that the LB films were Y-type, the alkyl chains were suggested to form a bilayer arrangement on each side of the coordination planes. A length of 1.54 nm, as estimated from an ideal all-*trans* conformation of the alkyl chains, would correspond to a calculated thickness of the sandwich layer of about 2.93 nm. The calculated mean tilting angle of the alkyl chains was determined to be about 18°, which would imply that there would only be a

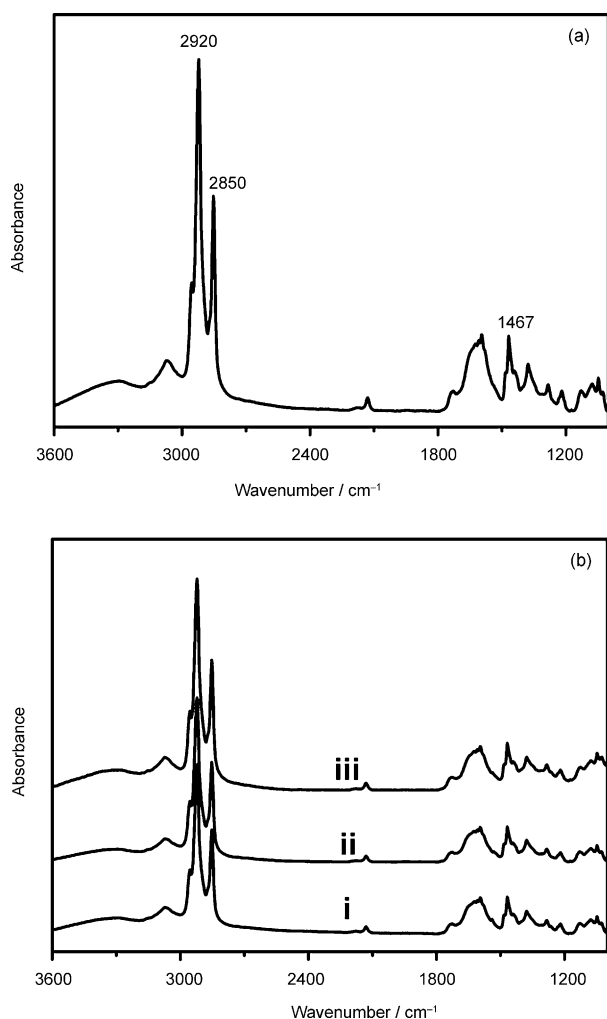


Figure 5. a) IR spectra of a 118-layer-thick LB film of complex **8** on a CaF₂ plate that was transferred at 35 mNm⁻¹ at 20°C. b) Polarized-IR spectra of a 118-layer-thick LB film of complex **8** on a CaF₂ plate that was transferred at 35 mNm⁻¹ at 20°C with incident angles of i) A_{||} (*i* = 0°), ii) A_⊥ (*i* = 0°), and iii) A_{||} (*i* = 60°).

very small angle between the Pt plane and the substrate. Thus, the calculated thickness of about 2.93 nm, which was essentially the same as the length of the alkyl chains in the bilayer, was in line with the layer thickness of 3.13 nm as obtained from the XRD measurements. Based on these structural properties, a possible packing model of the LB film is proposed in Figure 6. The deposition process onto a quartz plate of the LB film was monitored by electronic absorption spectroscopy. The absorbance was found to increase linearly with an increase in the number of deposition layers. The electronic absorption spectra of complexes **3-CI** and **8** in the LB films as a function of layer number are shown in Figure 7. The absorption patterns of the LB films of complexes **3-CI** (221, 245, 277, 329, 360, and 381 nm) and **8** (219, 256, 316, and 395 nm), were found to occur at similar energies to the corresponding complexes in solution. A linear relationship between the absorbance at 221 and 219 nm of complexes **3-CI** and **8**, respectively, and the number of

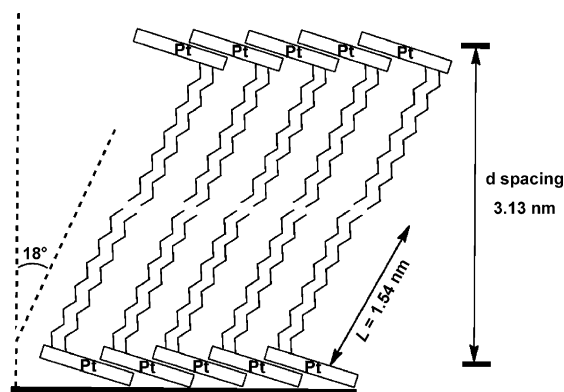


Figure 6. Schematic representation of the proposed packing structure of a LB film of complex **8**.

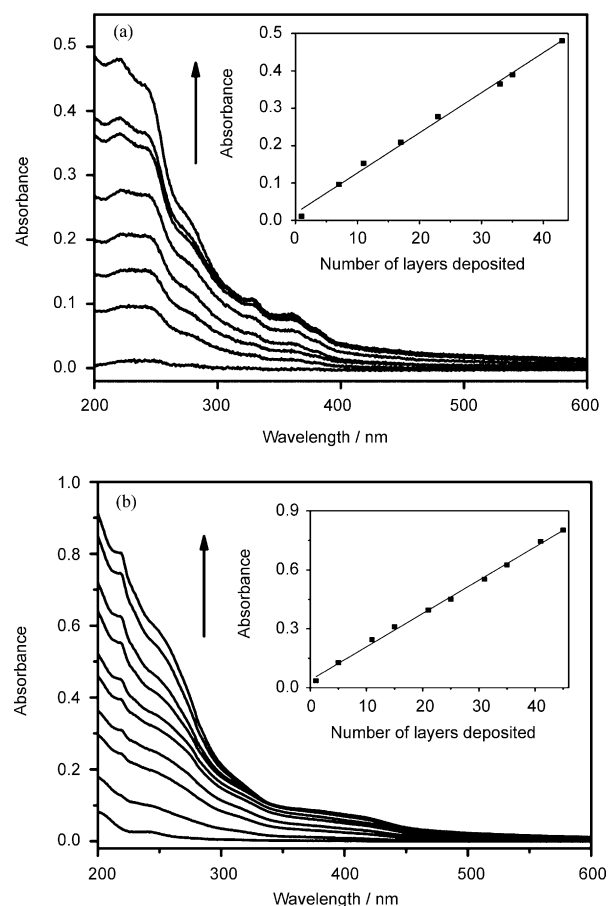


Figure 7. a) Electronic absorption spectra of LB films of complex **3-CI** with different numbers of layers that were deposited onto quartz at a surface pressure of 30 mNm⁻¹ (bottom to top: 1, 7, 11, 17, 23, 33, 35, and 43 layers). Inset: Plot of absorbance at 221 nm as a function of layer number. b) Electronic absorption spectra of LB films of complex **8** with different numbers of layers that were deposited onto quartz at a surface pressure of 35 mNm⁻¹ (bottom to top: 1, 5, 11, 15, 21, 25, 31, 35, 41, and 45 layers). Inset: Plot of absorbance at 219 nm as a function of layer number.

layers that were deposited onto the quartz substrate was obtained (Figure 7), thus suggesting stable and uniform LB film-forming properties of both complexes.

Apart from the study of their electrochemical, photophysical, and Langmuir–Blodgett film-formation properties, the complexes were also subjected to thermogravimetric analysis (TGA), polarized optical microscopy (POM), and differential scanning calorimetry (DSC) to confirm whether they could exist in liquid-crystalline phases. However, all of the complexes showed a lack of liquid-crystalline properties.

Conclusion

A new class of platinum(II) complexes of 2,6-bis(1-alkyl-1,2,3-triazol-4-yl)pyridine and 2,6-bis(1-aryl-1,2,3-triazol-4-yl)pyridine (N7R; R = *n*-C₄H₉, *n*-C₈H₁₇, *n*-C₁₂H₂₅, *n*-C₁₄H₂₉, *n*-C₁₈H₃₇, C₆H₅, and CH₂-C₆H₅), [Pt(N7R)Cl]X (**1–7**; X = OTf⁻ and PF₆⁻) and [Pt(N7R)(C≡CR')X] (**8–17**; X = OTf⁻, PF₆⁻, and Cl⁻; R' = C₆H₅, C₆H₄-CH₃-*p*, C₆H₄-CF₃-*p*, C₆H₄-N(CH₃)₂-*p*, and cholesteryl 2-propyn-1-yl carbonate), with different groups on the nitrogen atoms of the triazole units, has been synthesized and characterized. Their electrochemical and photophysical properties have also been studied. Two amphiphilic platinum(II) complexes of 2,6-bis(1-dodecyl-1,2,3-triazol-4-yl)pyridine (**3-Cl** and **8**) were found to form stable and reproducible LB films at the air/water interface. The characterization of such LB films has been investigated by studying their surface π–A isotherms, electronic absorption spectroscopy, XRD, and IR spectroscopy. The electronic absorption properties of complexes **3-Cl** and **8** in LB films have also been studied.

Experimental Section

Materials and reagents: Dichloro(1,5-cyclooctadiene)platinum(II) and cholesteryl chloroformate were purchased from Aldrich Chemical Co. Cholesteryl 2-propyn-1-yl carbonate was synthesized according to a literature procedure.^[4d] The 2,6-bis(1-alkyl-1,2,3-triazol-4-yl)pyridine and 2,6-bis(1-aryl-1,2,3-triazol-4-yl)pyridine ligands were synthesized from the click reactions of 2,6-diethynylpyridine with their corresponding aliphatic or aryl azides in the presence of a catalytic amount of copper(II) sulfate pentahydrate and sodium ascorbate, according to literature procedures.^[10] Chloroplatinum(II) complexes **1–7** were obtained by the modification of previously reported literature procedures for the synthesis of related platinum(II) complexes.^[6c,7a] Alkynylplatinum(II) complexes **8–17** were prepared by the reaction of their corresponding chloroplatinum(II) complexes with various organic alkynes in the presence of a catalytic amount of copper(I) iodide and triethylamine in CH₂Cl₂. Analytical-grade CHCl₃ was used as the spreading solvent for the studies of LB films and was distilled prior to use. Pure water (Milli-Pore, 18.2 MΩ) was employed for the LB-film-deposition experiments.

Synthesis of complex 1: A mixture of dichloro(1,5-cyclooctadiene)platinum(II) (120 mg, 0.32 mmol) and 2,6-bis(1-butyl-1,2,3-triazol-4-yl)pyridine (115 mg, 0.35 mmol) was heated at reflux in acetone/MeCN (2:1 v/v) overnight. After evaporation of the solvent, the residue was washed with Et₂O. A pale-yellow solid was obtained, which was dissolved in a minimum amount of MeOH and a metathesis reaction was performed to afford the hexafluorophosphate salt by using ammonium hexafluorophosphate. Subsequent recrystallization by the vapor diffusion of Et₂O into a solution of the product in MeCN/CH₂Cl₂ (3:1 v/v) gave complex **1** as a pale-yellow solid. Yield: 133 mg (59%); ¹H NMR (500 MHz, CD₃CN, 298 K, relative to SiMe₄): δ = 1.00 (t, *J* = 7.4 Hz, 6H; -CH₃), 1.40–1.47 (m, 4H; -CH₂-), 1.98–2.03 (m, 4H; -CH₂-), 4.60 (t, *J* = 7.2 Hz, 4H; -CH₂-),

8.00 (d, *J* = 8.0 Hz, 2H; pyridine), 8.37 (t, *J* = 8.0 Hz, 1H; pyridine), 8.67 ppm (s, 2H; triazole); positive FAB-MS: *m/z*: 556 [M–PF₆]⁺; elemental analysis calcd (%) for C₁₇H₂₃N₇F₆ClPPt: C 29.13, H 3.31, N 13.99; found: C 29.08, H 3.40, N 14.18.

Synthesis of complex 2: The procedure was similar to that for complex **1**, except that 2,6-bis(1-octyl-1,2,3-triazol-4-yl)pyridine (150 mg, 0.35 mmol) was used in place of 2,6-bis(1-butyl-1,2,3-triazol-4-yl)pyridine. Yield: 143 mg (55%); ¹H NMR (400 MHz, CD₃CN, 298 K, relative to SiMe₄): δ = 0.93 (t, *J* = 7.1 Hz, 6H; -CH₃), 1.35–1.45 (m, 20H; -(CH₂)₅-), 2.06–2.12 (m, 4H; -CH₂-), 4.60 (t, *J* = 7.4 Hz, 4H; -CH₂-), 8.00 (d, *J* = 8.1 Hz, 2H; pyridine), 8.15 (t, *J* = 8.1 Hz, 1H; pyridine), 8.67 ppm (s, 2H; triazole); positive FAB-MS: *m/z*: 667 [M–PF₆]⁺; elemental analysis calcd (%) for C₂₅H₃₉N₇F₆ClPPt: C 36.93, H 4.83, N 12.06; found: C 36.75, H 4.67, N 12.25.

Synthesis of complex 3: The procedure was similar to that for complex **1**, except that 2,6-bis(1-dodecyl-1,2,3-triazol-4-yl)pyridine (192 mg, 0.35 mmol) was used in place of 2,6-bis(1-butyl-1,2,3-triazol-4-yl)pyridine. Yield: 133 mg (45%); ¹H NMR (400 MHz, CDCl₃, 298 K, relative to SiMe₄): δ = 0.87 (t, *J* = 6.6 Hz, 6H; -CH₃), 1.27–1.38 (m, 36H; -(CH₂)₉-), 2.02–2.07 (m, 4H; -CH₂-), 4.57 (t, *J* = 7.6 Hz, 4H; -CH₂-), 7.88 (d, *J* = 8.0 Hz, 2H; pyridine), 8.10 (t, *J* = 8.0 Hz, 1H; pyridine), 8.62 ppm (s, 2H; triazole); positive FAB-MS: *m/z*: 780 [M–PF₆]⁺; elemental analysis calcd (%) for C₃₃H₅₅N₇F₆ClPPt: C 42.83, H 5.99, N 10.60; found: C 42.74, H 6.07, N 10.64.

Synthesis of complex 4: The procedure was similar to that for complex **1**, except that 2,6-bis(1-tetradecyl-1,2,3-triazol-4-yl)pyridine (212 mg, 0.35 mmol) was used in place of 2,6-bis(1-butyl-1,2,3-triazol-4-yl)pyridine. Yield: 141 mg (45%); ¹H NMR (500 MHz, CDCl₃, 298 K, relative to SiMe₄): δ = 0.87 (t, *J* = 6.6 Hz, 6H; -CH₃), 1.27–1.38 (m, 36H; -(CH₂)₉-), 2.02–2.07 (m, 4H; -CH₂-), 4.57 (t, *J* = 7.6 Hz, 4H; -CH₂-), 7.88 (d, *J* = 8.0 Hz, 2H; pyridine), 8.12 (t, *J* = 8.0 Hz, 1H; pyridine), 8.65 ppm (s, 2H; triazole); positive FAB-MS: *m/z*: 836 [M–PF₆]⁺; elemental analysis calcd (%) for C₃₇H₆₃N₇F₆ClPPt·1.5 CH₂Cl₂·0.5 CH₃CN: C 42.06, H 6.03, N 9.32; found: C 42.19, H 5.72, N 9.05.

Synthesis of complex 5: The procedure was similar to that for complex **1**, except that 2,6-bis(1-octadecyl-1,2,3-triazol-4-yl)pyridine (251 mg, 0.35 mmol) was used in place of 2,6-bis(1-butyl-1,2,3-triazol-4-yl)pyridine. Yield: 140 mg (40%); ¹H NMR (300 MHz, CDCl₃, 298 K, relative to SiMe₄): δ = 0.88 (t, *J* = 6.3 Hz, 6H; -CH₃), 1.25–1.37 (m, 60H; -(CH₂)₁₅-), 2.04–2.06 (m, 4H; -CH₂-), 4.57 (t, *J* = 7.6 Hz, 4H; -CH₂-), 7.89 (d, *J* = 8.1 Hz, 2H; pyridine), 8.14 (t, *J* = 8.1 Hz, 1H; pyridine), 8.76 ppm (s, 2H; triazole); positive FAB-MS: *m/z*: 948 [M–PF₆]⁺; elemental analysis calcd (%) for C₄₅H₇₉N₇F₆ClPPt: C 49.42, H 7.28, N 8.97; found: C 49.30, H 7.23, N 9.27.

Synthesis of complex 6: The procedure was similar to that for complex **1**, except that 2,6-bis(1-phenyl-1,2,3-triazol-4-yl)pyridine (127 mg, 0.35 mmol) was used in place of 2,6-bis(1-butyl-1,2,3-triazol-4-yl)pyridine. Yield: 72 mg (30%); ¹H NMR (300 MHz, [D₆]DMSO, 298 K, relative to SiMe₄): δ = 7.73–7.75 (m, 6H; -Ph), 7.96 (d, *J* = 7.6 Hz, 4H; -Ph), 8.24 (d, *J* = 7.8 Hz, 2H; pyridine), 8.62 (t, *J* = 7.8 Hz, 1H; pyridine), 10.00 ppm (s, 2H; triazole); positive FAB-MS: *m/z*: 596 [M–PF₆]⁺; elemental analysis calcd (%) for C₂₁H₁₅N₇F₆ClPPt: C 34.04, H 2.04, N 13.23; found: C 33.85, H 2.45, N 13.57.

Synthesis of complex 7: The procedure was similar to that for complex **1**, except that 2,6-bis(1-benzyl-1,2,3-triazol-4-yl)pyridine (138 mg, 0.35 mmol) was used in place of 2,6-bis(1-butyl-1,2,3-triazol-4-yl)pyridine. Yield: 238 mg (88%); ¹H NMR (500 MHz, CDCl₃, 298 K, relative to SiMe₄): δ = 5.48 (s, 4H; -CH₂-), 7.23–7.26 (m, 10H; -Ph), 7.96 (d, *J* = 8.0 Hz, 2H; pyridine), 8.12 (t, *J* = 8.0 Hz, 1H; pyridine), 8.20 ppm (s, 2H; triazole); positive FAB-MS: *m/z*: 624 [M–OTf]⁺; elemental analysis calcd (%) for C₂₄H₁₉N₇F₃ClO₃SPT: C 37.29, H 2.48, N 12.68; found: C 37.51, H 2.57, N 12.88.

Synthesis of complex 8: To a degassed solution of complex **3** (297 mg, 0.32 mmol) in DMF (8 mL) were added NEt₃ (0.5 mL), a catalytic amount of CuI (2 mg), and phenylacetylene (50 mg, 0.5 mmol). The resultant solution was stirred at RT overnight under a nitrogen atmosphere. To the resultant solution was added a minimum amount of acetone and a metathesis reaction was performed with LiCl to afford a yellow precipi-

tate. Subsequent recrystallization by the vapor diffusion of Et₂O into a solution of the product in CH₂Cl₂ gave the desired product. Yield: 31 mg (11%); ¹H NMR (400 MHz, MeOD, 298 K, relative to SiMe₄): δ = 0.88 (t, *J* = 6.8 Hz, 6H; -CH₃), 1.28–1.42 (m, 36H; -(CH₂)₉-), 2.04–2.07 (m, 4H; -CH₂-), 4.62 (t, *J* = 7.2 Hz, 4H; -CH₂-), 7.20 (t, *J* = 7.4 Hz, 1H; -Ph), 7.30 (t, *J* = 7.4 Hz, 2H; -Ph), 7.41 (d, *J* = 7.1 Hz, 2H; -Ph), 8.10 (d, *J* = 8.0 Hz, 2H; pyridine), 8.36 (t, *J* = 8.0 Hz, 1H; pyridine), 9.04 ppm (s, 2H; triazole); positive FAB-MS: *m/z*: 846 [M–Cl]⁺; elemental analysis calcd (%) for C₄₁H₆₀N₇ClPt·CH₂Cl₂: C 52.26, H 6.47, N 10.16; found: C 52.30, H 6.37, N 10.47.

Synthesis of complex 9: To a degassed solution of complex 7 (247 mg, 0.32 mmol) in DMF (8 mL) were added NEt₃ (0.5 mL), a catalytic amount of CuI (2 mg), and phenylacetylene (50 mg, 0.5 mmol). The resultant solution was stirred at RT overnight under a nitrogen atmosphere. To the resultant solution was added a minimum amount of MeOH and a metathesis reaction was performed with NH₄PF₆ to afford a yellow precipitate. Subsequent recrystallization by the vapor diffusion of Et₂O into a solution of the product in MeCN/CH₂Cl₂ (3:1 v/v) gave the desired product. Yield: 134 mg (50%); ¹H NMR (400 MHz, CD₃CN, 298 K, relative to SiMe₄): δ = 5.75 (s, 4H; -CH₂-), 7.23–7.26 (m, 1H; -Ph), 7.33 (d, *J* = 4.4 Hz, 4H; -Ph), 7.47–7.49 (m, 10H; -Ph), 7.96 (d, *J* = 8.1 Hz, 2H; pyridine), 8.29 (t, *J* = 8.1 Hz, 1H; pyridine), 8.59 ppm (s, 2H; triazole); positive FAB-MS: *m/z*: 689 [M–PF₆]⁺; elemental analysis calcd (%) for C₃₄H₂₄N₇F₆PPt·0.25 CH₂Cl₂: C 43.85, H 2.88, N 11.46; found: C 44.09, H 2.71, N 11.49.

Synthesis of complex 10: The procedure was similar to that for complex 9, except that 4-ethynyltoluene (58 mg, 0.50 mmol) was used in place of phenylacetylene. Yield: 122 mg (45%); ¹H NMR (400 MHz, CDCl₃, 298 K, relative to SiMe₄): δ = 2.35 (s, 3H; -CH₃), 5.75 (s, 4H; -CH₂-), 7.14 (d, *J* = 8.0 Hz, 2H; -Ph), 7.21 (d, *J* = 8.0 Hz, 2H; -Ph), 7.47–7.49 (m, 10H; -Ph), 7.96 (d, *J* = 8.1 Hz, 2H; pyridine), 8.29 (t, *J* = 8.1 Hz, 1H; pyridine), 8.59 ppm (s, 2H; triazole); positive FAB-MS: *m/z*: 703 [M–PF₆]⁺; elemental analysis calcd (%) for C₃₂H₂₆N₇F₆PPt·0.5 CH₂Cl₂: C 43.81, H 3.06, N 11.01; found: C 43.94, H 3.16, N 11.30.

Synthesis of complex 11: The procedure was similar to that for complex 9, except that 4-ethynyl-*α,α,α*-trifluorotoluene (85 mg, 0.50 mmol) was used in place of phenylacetylene. Yield: 124 mg (43%); ¹H NMR (400 MHz, CD₃CN, 298 K, relative to SiMe₄): δ = 5.75 (s, 4H; -CH₂-), 7.47–7.49 (m, 12H; -Ph), 7.63 (d, *J* = 8.2 Hz, 2H; -Ph), 7.97 (d, *J* = 8.1 Hz, 2H; pyridine), 8.31 (t, *J* = 8.1 Hz, 1H; pyridine), 8.60 ppm (s, 2H; triazole); positive FAB-MS: *m/z*: 757 [M–PF₆]⁺; elemental analysis calcd (%) for C₃₂H₂₃N₇F₉PPt·0.25 CH₂Cl₂: C 41.92, H 2.56, N 10.62; found: C 42.01, H 2.69, N 10.91.

Synthesis of complex 12: The procedure was similar to that for complex 9, except that 4-ethynyl-*N,N*-dimethylaniline (73 mg, 0.50 mmol) was used in place of phenylacetylene. Yield: 53 mg (19%); ¹H NMR (300 MHz, CD₃CN, 298 K, relative to SiMe₄): δ = 2.92 (s, 6H; -N(CH₃)₂), 5.76 (s, 4H; -CH₂-), 6.69 (d, *J* = 8.8 Hz, 2H; -Ph), 7.17 (d, *J* = 8.8 Hz, 2H; -Ph), 7.48–7.51 (m, 10H; -Ph), 7.95 (d, *J* = 8.0 Hz, 2H; pyridine), 8.28 (t, *J* = 8.0 Hz, 1H; pyridine), 8.59 ppm (s, 2H; triazole); positive FAB-MS: *m/z*: 732 [M–PF₆]⁺; elemental analysis calcd (%) for C₃₃H₂₉N₈F₆PPt·1.5 CH₂Cl₂·CH₃CN: C 41.95, H 3.38, N 12.07; found: C 41.96, H 3.19, N 12.01.

Synthesis of complex 13: To a degassed solution of complex 1 (120 mg, 0.17 mmol) in DMF (8 mL) were added NEt₃ (0.5 mL), a catalytic amount of CuI (2 mg), and phenylacetylene (50 mg, 0.5 mmol). The resultant solution was stirred at RT overnight under a nitrogen atmosphere. Subsequent recrystallization by the vapor diffusion of Et₂O into a solution of the product in MeCN/CH₂Cl₂ (3:1 v/v) gave the desired product. Yield: 78 mg (60%); ¹H NMR (400 MHz, CD₃CN, 298 K, relative to SiMe₄): δ = 0.98 (t, *J* = 7.4 Hz, 6H; -CH₃), 1.39–1.46 (m, 4H; -CH₂-), 1.96–2.01 (m, 4H; -CH₂-), 4.58 (t, *J* = 7.3 Hz, 4H; -CH₂-), 7.25 (m, 3H; -Ph), 7.35 (m, 2H; -Ph), 8.01 (d, *J* = 8.0 Hz, 2H; pyridine), 8.35 (t, *J* = 8.0 Hz, 1H; pyridine), 8.63 ppm (s, 2H; triazole); positive FAB-MS: *m/z*: 621 [M–PF₆]⁺; elemental analysis calcd (%) for C₂₃H₂₈N₅F₆PPt·0.25 CH₂Cl₂: C 38.49, H 3.65, N 12.45; found: C 38.06, H 3.55, N 12.64.

Synthesis of complex 14: The procedure was similar to that for complex 13, except that cholesteryl 2-propyn-1-yl carbonate (170 mg, 0.36 mmol) was used in place of phenylacetylene. To the resultant solution was added CH₂Cl₂ and the mixture was filtered. After removal of most of the solvent, MeOH was added and a yellow precipitate was obtained. The solid was washed three times each with MeOH and *n*-hexane. The crude product was re-dissolved in acetone and was filtered. After removal of solvent from the filtrate, the desired product was obtained as a yellow solid. Yield: 86 mg (27%); ¹H NMR (400 MHz, CDCl₃, 298 K, relative to SiMe₄): δ = 0.69 (s, 3H; cholesteryl proton), 0.86–0.88 (m, 6H; cholesteryl proton), 0.92 (d, *J* = 6.4 Hz, 3H; cholesteryl proton), 0.97 (t, *J* = 7.3 Hz, 6H; -CH₃), 0.95–1.52 (m, 28H; -CH₂-, cholesteryl proton), 1.81–2.09 (m, 9H; -CH₂-, cholesteryl proton), 2.41–2.45 (m, 2H; cholesteryl proton), 4.51–4.58 (m, 5H; -OCH₂-, -NCH₂-), 5.18 (s, 2H; -OCH₂C≡C-), 5.40 (d, *J* = 5.2 Hz, 1H; -HC=C-), 7.85 (d, *J* = 8.0 Hz, 2H; pyridine), 7.95 (t, *J* = 8.0 Hz, 1H; pyridine), 8.65 ppm (s, 2H; triazole); positive FAB-MS: *m/z*: 987 [M–PF₆]⁺; elemental analysis calcd (%) for C₄₈H₇₀N₇F₆O₃PPt: C 50.88, H 6.23, N 8.65; found: C 50.45, H 6.14, N 8.27.

Synthesis of complex 15: The procedure was similar to that for complex 14, except that complex 2 (146 mg, 0.18 mmol) was used in place of complex 1. Yield: 53 mg (23%); ¹H NMR (400 MHz, CDCl₃, 298 K, relative to SiMe₄): δ = 0.69 (s, 3H; cholesteryl proton), 0.84–0.88 (m, 12H; -CH₃, cholesteryl proton), 0.92 (d, *J* = 6.5 Hz, 3H; cholesteryl proton), 0.95–1.58 (m, 44H; -(CH₂)₅-, cholesteryl proton), 1.82–2.03 (m, 9H; -CH₂-, cholesteryl proton), 2.41–2.45 (m, 2H; cholesteryl proton), 4.51–4.58 (m, 1H; -OCH₂-), 4.70 (t, *J* = 7.0 Hz, 4H; -NCH₂-), 5.05 (s, 2H; -OCH₂C≡C-), 5.42 (d, *J* = 5.0 Hz, 1H; -HC=C-), 7.85 (d, *J* = 8.0 Hz, 2H; pyridine), 7.95 (t, *J* = 8.0 Hz, 1H; pyridine), 8.65 ppm (s, 2H; triazole); positive FAB-MS: *m/z*: 1100 [M–PF₆]⁺; elemental analysis calcd (%) for C₅₆H₈₆N₇F₆O₃PPt·C₆H₁₄·0.5 CH₂Cl₂: C 54.63, H 7.41, N 7.13; found: C 54.68, H 7.24, N 6.98.

Synthesis of complex 16: The procedure was similar to that for complex 14, except that complex 3 (180 mg, 0.19 mmol) was used in place of complex 1. Yield: 54 mg (21%); ¹H NMR (400 MHz, CDCl₃, 298 K, relative to SiMe₄): δ = 0.69 (s, 3H; cholesteryl proton), 0.84–0.88 (m, 12H; -CH₃, cholesteryl proton), 0.92 (d, *J* = 6.5 Hz, 3H; cholesteryl proton), 0.95–1.60 (m, 60H; -(CH₂)₉-, cholesteryl proton), 1.83–2.04 (m, 9H; -CH₂-, cholesteryl proton), 2.42–2.44 (m, 2H; cholesteryl proton), 4.49–4.57 (m, 1H; -OCH₂-), 4.70 (t, *J* = 7.0 Hz, 4H; -NCH₂-), 5.05 (s, 2H; -OCH₂C≡C-), 5.42 (d, *J* = 5.0 Hz, 1H; -HC=C-), 7.85 (d, *J* = 8.0 Hz, 2H; pyridine), 7.95 (t, *J* = 8.0 Hz, 1H; pyridine), 8.65 ppm (s, 2H; triazole); positive FAB-MS: *m/z*: 1211 [M–PF₆]⁺; elemental analysis calcd (%) for C₆₄H₁₀₂N₇F₆O₃PPt: C 56.62, H 7.57, N 7.22; found: C 56.88, H 7.43, N 7.14.

Synthesis of complex 17: The procedure was similar to that for complex 14, except that complex 5 (393 mg, 0.36 mmol) was used in place of complex 1. Yield: 84 mg (15%); ¹H NMR (400 MHz, CDCl₃, 298 K, relative to SiMe₄): δ = 0.69 (s, 3H; cholesteryl proton), 0.84–0.88 (m, 12H; -CH₃, cholesteryl proton), 0.92 (d, *J* = 6.5 Hz, 3H; cholesteryl proton), 0.93–1.62 (m, 84H; -(CH₂)₁₅-, cholesteryl proton), 1.83–2.04 (m, 9H; -CH₂-, cholesteryl proton), 2.42–2.44 (m, 2H; cholesteryl proton), 4.49–4.57 (m, 1H; -OCH₂-), 4.70 (t, *J* = 7.0 Hz, 4H; -NCH₂-), 5.05 (s, 2H; -OCH₂C≡C-), 5.42 (d, *J* = 5.0 Hz, 1H; -HC=C-), 7.85 (d, *J* = 8.0 Hz, 2H; pyridine), 7.95 (t, *J* = 8.0 Hz, 1H; pyridine), 8.65 ppm (s, 2H; triazole); positive FAB-MS: *m/z*: 1379 [M–PF₆]⁺; elemental analysis calcd (%) for C₇₆H₁₂₆N₇F₆O₃PPt·CH₂Cl₂: C 57.43, H 8.01, N 6.10; found: C 57.31, H 7.93, N 6.43.

Preparation of complex 3-Cl: To a solution of complex 3 in acetone was added a solution of LiCl in acetone and a yellow precipitate was obtained. Subsequent recrystallization by the vapor diffusion of Et₂O into a solution of the product in CH₂Cl₂ gave complex 3-Cl.

Preparation of the LB films: A Nima 622D trough that was equipped with a Wilhelmy balance as a surface-pressure sensor was employed for the surface-pressure-molecular-area isotherm measurements and for the deposition of the LB films. Solutions of complexes 3-Cl and 8 in CHCl₃ (1 mg mL⁻¹) were prepared. After spreading the sample solution over the water subphase, the monolayer was kept at the air/water interface for 20 min to allow the complete evaporation of the solvent and then compressed at a constant barrier rate of 20 cm² min⁻¹. The temperature of the

subphase was kept at $(20 \pm 0.5)^\circ\text{C}$. All of the isotherms were repeated at least three times. Then, the Langmuir monolayer was allowed to stabilize for 15 min at the target pressure and the condensed monolayer was finally transferred by the “vertical-dipping” method onto a quartz substrate for the electronic absorption and XRD measurements or onto a CaF_2 substrate for the IR and polarized-IR measurements. In all cases, the dipping rate was 6 mm min^{-1} . The transfer ratios were reproducible and approached unity (0.9–1.0) in the repeated deposition cycles.

Physical measurements and instrumentation: ^1H NMR spectra were recorded on Bruker DPX 400 FT-NMR spectrometer (400 MHz) or Bruker Avance 500 instruments (500 MHz) at 298 K; chemical shifts are reported relative to tetramethylsilane (SiMe_4). All positive-ion FAB and EI mass spectra were recorded on a Finnigan MAT95 mass spectrometer. Elemental analysis was performed on a Flash EA1112 from ThermoQuest Italia SPA at the Changchun Institute of Applied Chemistry or on a Carlo Erba 1106 elemental analyzer at the Institute of Chemistry, Chinese Academy of Sciences.

Cyclic voltammetry measurements were performed on a CH Instruments, Inc. model CHI 600A electrochemical analyzer. The electrolytic cell was a conventional two-compartment cell. Electrochemical measurements were performed in MeCN with $0.1 \text{ M } n\text{Bu}_4\text{NPF}_6$ as a supporting electrolyte at RT. The reference electrode was a Ag/AgNO_3 (0.1 M in MeCN) electrode, the working electrode was a glassy carbon electrode (CH Instruments, Inc.), and the counter electrode with a platinum wire. First, the surface of the working electrode was polished on a microcloth with a $1 \mu\text{m}$ alumina slurry (Linde), followed by a $0.3 \mu\text{m}$ alumina slurry (Buehler Co.). Treatment of the electrode surface was performed according to a literature procedure.^[16] The ferrocenium/ferrocene couple ($\text{Fc}^{\text{p}+}/\text{Fc}^{\text{0}}$) was used as an internal reference.^[17] All of the solutions for the electrochemical studies were deaerated with pre-purified argon gas just prior to the measurements.

The electronic absorption spectra were obtained on a Hewlett–Packard 8452A diode-array spectrophotometer or on a Shimadzu 3100 PC spectrophotometer. Steady-state excitation and emission spectra were recorded at RT on a Spex Fluorolog-2 Model F111 fluorescence spectrofluorometer that was equipped with a Hamamatsu R-928 photomultiplier tube. All of the solutions for the photophysical studies were prepared under high vacuum in a 10 cm^3 round-bottomed flask that was equipped with a 1 cm sidearm fluorescence cuvette and sealed from the atmosphere with a Rotaflo HP6/6 quick-release Teflon stopper. Solutions were rigorously degassed on a high-vacuum line in a two-compartment cell by no less than four successive freeze-pump-thaw cycles. For the solid-state photophysical measurements, the solid sample was loaded into a quartz tube inside a quartz-walled Dewar flask. Liquid nitrogen was placed into the Dewar flask for the low-temperature (77 K) photophysical measurements. Excited-state lifetimes of the solution samples were measured by using a conventional laser system. The excitation source was the 355 nm output (third harmonic, 8 ns) of a Spectra-Physics Quanta-Ray Q-switched GCR-150 pulsed Nd:YAG laser (10 Hz). Luminescence decay signals were detected by a Hamamatsu R928 PMT on a Tektronix model TDS-620A (500 MHz, 2 GSs^{-1}) digital oscilloscope and analyzed by using a program for the exponential fits.

XRD was performed on a Rigaku X-ray diffractometer (D/max-rA, $\text{Cu}_{\text{K}\alpha}$ radiation, $\lambda = 1.542 \text{ \AA}$) and the data were collected from 0.7 – 10° . FTIR spectroscopy was performed on a Bruker VERTEX 80 V FTIR spectrometer that was equipped with a mercury-cadmium-telluride (MCT) detector (256 scans) at a resolution of 4 cm^{-1} . Polarized-IR measurements were performed at incident angles of 0 and 60° , respectively, by using a polarizer attachment.

Thermogravimetric analysis (TGA) was performed on a Perkin–Elmer Diamond TG/DTA instrument at a heating rate of $10^\circ\text{C min}^{-1}$. Differential scanning calorimetry (DSC) measurements were performed on a Netzsch DSC 204. The scan rate was 5°C min^{-1} . The samples were sealed in aluminum capsules in air and the holder was placed under an atmosphere of dry nitrogen. Polarized optical micrographs were obtained on a Zeiss Axioskop 40 polarizing microscope that was equipped with a Linkam THMSE 600 hot stage, a central processor, and a DF1 cooling system.

Acknowledgements

We acknowledge support from The University of Hong Kong under the URC Strategic Research Theme on New Materials, the State Key Laboratory of Supramolecular Structure and Materials, Jilin University, and The University of Hong Kong. This work was supported by the National Basic Research Program of China (973 Program; 2013CB834701), the General Research Fund (GRF) (HKU 7063/10P) and the University Grants Committee Areas of Excellence Scheme (AoE/P-03/08).

- [1] a) R. S. Osborn, D. Rogers, *J. Chem. Soc. Dalton Trans.* **1974**, 1002; b) R. H. Herber, M. Croft, M. J. Coyer, B. Bilash, A. Sahiner, *Inorg. Chem.* **1994**, *33*, 2422; c) W. B. Connick, R. E. Marsh, W. P. Schaefer, H. B. Gray, *Inorg. Chem.* **1997**, *36*, 913; d) V. M. Miskowski, V. H. Houlding, C.-M. Che, Y. Wang, *Inorg. Chem.* **1993**, *32*, 2518; e) W. B. Connick, D. Geiger, R. Eisenberg, *Inorg. Chem.* **1999**, *38*, 3264; f) F. Hua, S. Kinayyigit, J. R. Cable, F. N. Castellano, *Inorg. Chem.* **2005**, *44*, 471; g) C. Ed. Whittle, J. A. Weinstein, M. W. George, K. S. Schanze, *Inorg. Chem.* **2001**, *40*, 4053; h) M. Hissler, W. B. Connick, D. K. Geiger, J. E. McGarrah, D. Lipa, R. J. Lachicotte, R. Eisenberg, *Inorg. Chem.* **2000**, *39*, 447; i) C.-M. Che, L.-Y. He, C.-K. Poon, T. C.-W. Mak, *Inorg. Chem.* **1989**, *28*, 3081.
- [2] a) V. W.-W. Yam, R. P.-L. Tang, K. M.-C. Wong, K.-K. Cheung, *Organometallics* **2001**, *20*, 4476; b) V. W.-W. Yam, K. M.-C. Wong, N. Zhu, *J. Am. Chem. Soc.* **2002**, *124*, 6506; c) V. W.-W. Yam, K. H.-Y. Chan, K. M.-C. Wong, N. Zhu, *Chem. Eur. J.* **2005**, *11*, 4535; d) C. Yu, K. M.-C. Wong, K. H.-Y. Chan, V. W.-W. Yam, *Angew. Chem.* **2005**, *117*, 801; *Angew. Chem. Int. Ed.* **2005**, *44*, 791; e) C. Yu, K. H.-Y. Chan, K. M.-C. Wong, V. W.-W. Yam, *Chem. Eur. J.* **2008**, *14*, 4577; f) C. Yu, K. H.-Y. Chan, K. M.-C. Wong, V. W.-W. Yam, *Proc. Natl. Acad. Sci. USA* **2006**, *103*, 19657; g) V. W.-W. Yam, K. H.-Y. Chan, K. M.-C. Wong, B. W.-K. Chu, *Angew. Chem.* **2006**, *118*, 6315; *Angew. Chem. Int. Ed.* **2006**, *45*, 6169; h) A. Y.-Y. Tam, K. M.-C. Wong, V. W.-W. Yam, *Chem. Eur. J.* **2009**, *15*, 4775; i) K. H.-Y. Chan, J. W.-Y. Lam, K. M.-C. Wong, B.-Z. Tang, V. W.-W. Yam, *Chem. Eur. J.* **2009**, *15*, 2328; j) C. Po, A. Y.-Y. Tam, K. M.-C. Wong, V. W.-W. Yam, *J. Am. Chem. Soc.* **2011**, *133*, 12136; k) S. Y.-L. Leung, A. Y.-Y. Tam, C.-H. Tao, H.-S. Chow, V. W.-W. Yam, *J. Am. Chem. Soc.* **2012**, *134*, 1047; l) C. Y.-S. Chung, V. W.-W. Yam, *J. Am. Chem. Soc.* **2011**, *133*, 18775; m) C. Y.-S. Chung, V. W. W. Yam, *Chem. Sci.* **2013**, *4*, 337; n) K. M.-C. Wong, V. W.-W. Yam, *Acc. Chem. Res.* **2011**, *44*, 424; o) A. Y.-Y. Tam, V. W.-W. Yam, *Chem. Soc. Rev.* **2013**, *42*, 1540; p) V. W.-W. Yam, K. M.-C. Wong, *Chem. Commun.* **2011**, *47*, 11579; q) K. H.-Y. Chan, H.-S. Chow, K. M.-C. Wong, M. C.-L. Yeung, V. W.-W. Yam, *Chem. Sci.* **2010**, *1*, 477.
- [3] a) H.-K. Yip, L.-K. Cheng, K.-K. Cheung, C.-M. Che, *J. Chem. Soc. Dalton Trans.* **1993**, 2933; b) J. A. Bailey, M. G. Hill, R. E. Marsh, V. M. Miskowski, W. P. Schaefer, H. B. Gray, *Inorg. Chem.* **1995**, *34*, 4591; c) R. Büchner, J. S. Field, R. J. Haines, *Inorg. Chem.* **1997**, *36*, 3952; d) J. Moussa, K. M.-C. Wong, L.-M. Chamoreau, H. Amouri, V. W.-W. Yam, *Dalton Trans.* **2007**, 3526; e) T. K. Aldridge, E. M. Stacy, D. R. McMillin, *Inorg. Chem.* **1994**, *33*, 722; f) T. J. Wadas, Q. M. Wang, Y. J. Kim, C. Flaschenreim, T. N. Blanton, R. Eisenberg, *J. Am. Chem. Soc.* **2004**, *126*, 16841; g) K. W. Jennette, J. T. Gill, J. A. Sadowick, S. J. Lippard, *J. Am. Chem. Soc.* **1976**, *98*, 6159; h) S.-W. Lai, M. C.-W. Chan, K.-K. Cheung, C.-M. Che, *Inorg. Chem.* **1999**, *38*, 4262; i) J. A. Bailey, V. M. Miskowski, H. B. Gray, *Inorg. Chem.* **1993**, *32*, 369; j) M. G. Hill, J. A. Bailey, V. M. Miskowski, H. B. Gray, *Inorg. Chem.* **1996**, *35*, 4585; k) R. Büchner, C. T. Cunningham, J. S. Field, R. J. Haines, D. R. McMillin, G. C. Summerton, *J. Chem. Soc. Dalton Trans.* **1999**, 711; l) G. Arena, G. Calogero, S. Campagna, L. M. Scolaro, V. Ricevuto, R. Romeo, *Inorg. Chem.* **1998**, *37*, 2763; m) J. F. Michalec, S. A. Bejune, D. R. McMillin, *Inorg. Chem.* **2000**, *39*, 2708; n) D. K. Crites, C. T. Cunningham, D. R. McMillin, *Inorg. Chim. Acta* **1998**, *273*, 346.
- [4] a) A. Y.-Y. Tam, K. M.-C. Wong, G. Wang, V. W.-W. Yam, *Chem. Commun.* **2007**, 2028; b) A. Y.-Y. Tam, K. M.-C. Wong, N. Zhu, G. Wang, V. W.-W. Yam, *Langmuir* **2009**, *25*, 8685; c) A. Y.-Y. Tam,

- K. M.-C. Wong, V. W.-W. Yam, *J. Am. Chem. Soc.* **2009**, *131*, 6253; d) Y. Li, A. Y.-Y. Tam, K. M.-C. Wong, W. Li, L. Wu, V. W.-W. Yam, *Chem. Eur. J.* **2011**, *17*, 8048; e) K.-C. Chang, J.-L. Lin, Y.-T. Shen, C.-Y. Hung, C.-Y. Chen, S.-S. Sun, *Chem. Eur. J.* **2012**, *18*, 1312; f) F. Camerel, R. Ziessel, B. Donnio, C. Bourgogne, D. Guillon, M. Schmutz, C. Iacovita, J. P. Bucher, *Angew. Chem.* **2007**, *119*, 2597; *Angew. Chem. Int. Ed.* **2007**, *46*, 2545; g) T. Tu, W. Fang, X. Bao, X. Li, K. H. Dötz, *Angew. Chem.* **2011**, *123*, 6731; *Angew. Chem. Int. Ed.* **2011**, *50*, 6601.
- [5] a) W.-S. Tang, X. Lu, K. M.-C. Wong, V. W.-W. Yam, *J. Mater. Chem.* **2005**, *15*, 2714; b) H.-S. Lo, S.-K. Yip, K. M.-C. Wong, N. Zhu, V. W.-W. Yam, *Organometallics* **2006**, *25*, 3537; c) Q. Z. Yang, Q. X. Tong, L. Z. Wu, Z. X. Wu, L. P. Zhang, C. H. Tung, *Eur. J. Inorg. Chem.* **2004**, 1948; d) K. M.-C. Wong, W.-S. Tang, X. Lu, N. Zhu, V. W.-W. Yam, *Inorg. Chem.* **2005**, *44*, 1492; e) X. Han, L. Z. Wu, G. Si, J. Pan, Q. Z. Yang, L. P. Zhang, C. H. Tung, *Chem. Eur. J.* **2007**, *13*, 1231; f) H.-S. Lo, S.-K. Yip, N. Zhu, V. W.-W. Yam, *Dalton Trans.* **2007**, 4386; g) K. M.-C. Wong, W.-S. Tang, B. W.-K. Chu, N. Zhu, V. W.-W. Yam, *Organometallics* **2004**, *23*, 3459; h) S. Chakraborty, T. J. Wadas, H. Hester, C. Flaschenreim, R. Schmehl, R. Eisenberg, *Inorg. Chem.* **2005**, *44*, 6284.
- [6] a) K. Wang, M. A. Haga, H. Monjushiro, M. Akiba, Y. Sasaki, *Inorg. Chem.* **2000**, *39*, 4022; b) L. J. Grove, J. M. Rennekamp, H. Jude, W. B. Connick, *J. Am. Chem. Soc.* **2004**, *126*, 1594; c) E. J. Rivera, C. Figueroa, J. L. Colón, L. Grove, W. B. Connick, *Inorg. Chem.* **2007**, *46*, 8569; d) V. G. Vaidyanathan, B. U. Nair, *Eur. J. Inorg. Chem.* **2005**, 3756; e) A. Y.-Y. Tam, W.-H. Lam, K. M.-C. Wong, N. Zhu, V. W.-W. Yam, *Chem. Eur. J.* **2008**, *14*, 4562.
- [7] a) L. Zhao, K. M.-C. Wong, B. Li, W. Li, N. Zhu, L. Wu, V. W.-W. Yam, *Chem. Eur. J.* **2010**, *16*, 6797; b) C.-M. Che, C.-F. Chow, M.-Y. Yuen, V. A.-L. Roy, W. Lu, Y. Chen, S. S.-Y. Chui, N. Zhu, *Chem. Sci.* **2011**, *2*, 216.
- [8] S. A. Willison, H. Jude, R. M. Antonelli, J. M. Rennekamp, N. A. Eckert, J. A. K. Bauer, W. B. Connick, *Inorg. Chem.* **2004**, *43*, 2548.
- [9] a) R. M. Meudtner, S. Hecht, *Macromol. Rapid Commun.* **2008**, *29*, 347; b) R. M. Meudtner, M. Ostermeier, R. Goddard, C. Limberg, S. Hecht, *Chem. Eur. J.* **2007**, *13*, 9834; c) M. Ostermeier, M. A. Berlin, R. M. Meudtner, S. Demeshko, F. Meyer, C. Limberg, S. Hecht, *Chem. Eur. J.* **2010**, *16*, 10202.
- [10] Y. Li, J. C. Huffmanab, A. H. Flood, *Chem. Commun.* **2007**, 2692.
- [11] a) B. Schulze, C. Friebe, S. Hoepfner, G. M. Pavlov, A. Winter, M. D. Hager, U. S. Schubert, *Macromol. Rapid Commun.* **2012**, *33*, 597; b) B. Schulze, C. Friebe, M. D. Hager, A. Winter, R. Hoogenboom, H. Görls, U. S. Schubert, *Dalton Trans.* **2009**, 787.
- [12] a) H. L. Casal, D. G. Cameron, H. H. Mantsch, *J. Phys. Chem.* **1985**, *89*, 5557; b) W. Li, S. Yi, Y. Wu, L. Wu, *J. Phys. Chem. B* **2006**, *110*, 16961.
- [13] R. A. MacPhail, H. L. Strauss, R. G. Snyder, C. A. Elliger, *J. Phys. Chem.* **1984**, *88*, 334.
- [14] H. Hagemann, R. G. Snyder, A. J. Peacock, L. Mandelkern, *Macromolecules* **1989**, *22*, 3600.
- [15] J. J. Benítez, S. Kopta, D. F. Ogletree, M. Salmeron, *Langmuir* **2002**, *18*, 6096.
- [16] C.-M. Che, K.-Y. Wong, F.-C. Anson, *J. Electroanal. Chem. Interfacial Electrochem.* **1987**, *226*, 211.
- [17] N. G. Connelly, W. E. Geiger, *Chem. Rev.* **1996**, *96*, 877.

Received: May 10, 2013

Published online: September 16, 2013